JBC ARTICLE

Phosphorylated immunoreceptor tyrosine-based activation motifs and integrin cytoplasmic domains activate spleen tyrosine kinase via distinct mechanisms

Lina Antenucci[‡1], Vesa P. Hytönen[§], and Jari Ylänne[‡]

From the ‡Department of Biological and Environmental Science and Nanoscience Center, University of Jyväskylä, Survontie 9 C, 40014 Jyväskylä, Finland and the §Faculty of Medicine and Life Sciences and BioMediTech, University of Tampere, and Fimlab Laboratories, Tampere 33014, Finland

Edited by John M. Denu

Spleen tyrosine kinase (Syk) is involved in cellular adhesion and also in the activation and development of hematopoietic cells. Syk activation induced by genomic rearrangement has been linked to certain T-cell lymphomas, and Syk inhibitors have been shown to prolong survival of patients with B-cell lineage malignancies. Syk is activated either by its interaction with a double-phosphorylated immunoreceptor tyrosine-based activation motif (pITAM), which induces rearrangements in the Syk structure, or by the phosphorylation of specific tyrosine residues. In addition to its immunoreceptor function, Syk is activated downstream of integrin pathways, and integrins bind to the same region in Syk as does pITAM. However, it is unknown whether integrins and pITAM use the same mechanism to activate Syk. Here, using purified Syk protein and fluorescence-based enzyme assay we investigated whether interaction of the integrin β_3 cytoplasmic domain with the Syk regulatory domain causes changes in Syk activity similar to those induced by pITAM peptides. We observed no direct Syk activation by soluble integrin peptide, and integrin did not compete with pITAM-induced activation even though at high concentrations, the integrin cytoplasmic domain peptide competed with Syk's substrate. However, clustered integrin peptides induced Syk activation, presumably via a transphosphorylation mechanism. Moreover, the clustered integrins also activated a Syk variant in which tyrosines were replaced with phenylalanine (Y348F/Y352F), indicating that clustered integrin–induced Syk activation involved other phosphorylation sites. In conclusion, integrin cytoplasmic domains do not directly induce Syk conformational changes and do not activate Syk via the same mechanism as pITAM.

Spleen tyrosine kinase (Syk) is a 72-kDa cytoplasmic signaling protein discovered in bovine thymus (1) and forms a small family of non-receptor tyrosine kinases with ζ chain-associated protein kinase of 70 kDa (ZAP-70) (2). Knockout studies in

mouse show that Syk is required for B-cell differentiation (3). $Syk^{-/-}$ mice are not viable because of severe perinatal hemorrhage due to lack of separation of lymphatic and venous vasculature (4). Even though $Syk^{-/-}$ stem cells can give rise to all other hematopoietic cells than B-cells, Syk seems to have a wide function in many hematopoietic cell types, whereas the function of ZAP-70 is more restricted to T-cell and NK cells (2).

Syk has an important role in cancer. In hematological malignancies Syk is mainly considered as a tumor promoter (5). A chromosomal translocation has been found in T-cell leukemias leading to fusion of interleukin 2 inducible T-cell kinase (*ITK*) and *SYK* genes and to an aberrantly active Syk kinase (6). This fusion has been validated as an oncogenic driver in a mouse model (7). In many other hematological malignancies high Syk activity has been detected (5), although, to our knowledge, no human point mutations have been validated as oncogenic driver mutations. Small molecule Syk inhibitors have been designed and they were shown to prolong survival of patients (8). At the moment, Syk inhibitors have not been approved for clinical use because they are rather nonspecific and many side effects are observed (9). In solid tumors, the role of Syk is less clear than in hematological tissues. In many cases *SYK* expression is reduced during malignancy (*e.g.* see Ref. 10, reviewed in Ref. 5). Many somatic mutations have been found in *SYK* genes (cancer.sanger.ac.uk/cosmic)[2] and epigenetic modification can also be responsible for alterations in the expression (11). There is some evidence that Syk can act as a tumor suppressor in breast carcinomas because it reduces cell growth when re-expressed in a breast carcinoma cell line and tested in a xeno-transplantation model (12).

Syk has a C-terminal tyrosine kinase domain and an N-terminal regulatory domain formed by two Src homology 2 (SH2)[3] domains connected by a flexible linker region called interdomain A (IA). This tandem SH2 region (tSH2) is connected to the kinase domain via a second linker region called interdomain B (IB) (13). The Syk activation mechanism is mostly understood. The inactive kinase can interact through SH2 domains

[2] Please note that the JBC is not responsible for the long-term archiving and maintenance of this site or any other third party hosted site.
[3] The abbreviations used are: SH2, Src homology 2; tSH2, tandem SH2; IA, interdomain A; IB, interdomain B; pITAM, phosphorylated immunoreceptor tyrosine-based activation motif; SPR, surface plasmon resonance; TEV, tobacco etch virus; RU, response unit; ANOVA, analysis of variance.

with phosphorylated immunoreceptor tyrosine-based activation motif (pITAM) associated with TCR, BCR, and FcR receptors. Upon pITAM binding the tSH2 of Syk changes its orientation in relationship to the kinase domain and allows kinase activity (13). In addition, Syk is phosphorylated by Lyn and Lck kinases and it also has an auto/transphosphorylation activity that can lead to Syk activation independently from pITAM (14). Considering that, an "OR gate switch" model for Syk activation has been proposed (14, 15). This means that an initial activation by either pITAM binding, OR, by a phosphorylation event can ultimately lead to full activity of the enzyme.

In many different biological processes ITAM-based receptor signaling is concomitant with integrin signaling. The classical example of this kind of collaboration is immunological synapse, where both β_2 integrins and TCR are required (16, 17). In neutrophils FcR signaling is linked to both integrin β_2 and β_3 function (18, 19). During platelet adhesion to damaged vascular cell wall the collagen receptor GPVI–FcRγ complex works in concert with β_1 and β_3 integrins (20). Clearly there are multiple crossing points between pITAM/Syk and integrin signaling pathways (reviewed in Ref. 2). There is also a direct interaction between Syk and integrins: Syk interacts with integrin β_1, β_2, and β_3 cytoplasmic tails (21) and the interaction is mediated mainly by N-SH2 domain and IA, whereas the C-SH2 has only a marginal role in the binding (22). On the integrin side, the last 23 amino acids of β_3 are sufficient for binding to Syk and deletion of four C-terminal residues abolished the binding (21). There are two tyrosine residues in the Syk interacting sequence of integrin β_3, but the interaction does not require integrin phosphorylation. Rather, tyrosine-phosphorylated integrin tails fail to interact with Syk (22). Although Syk has been shown to be required for normal $\alpha_{IIb}\beta_3$ integrin function in platelets (23), a recent study has shown that integrin-induced Syk signaling is independent on pITAM-induced Syk activation (24). In this study, mutation of the Syk N-SH2 domain that prevented phosphotyrosine binding blocked ITAM-dependent signaling in mouse platelet, but did not alter integrin-dependent Syk activation (24).

Even though integrins were found to activate Syk signaling more than two decades ago (25), it is still unclear how this activation works. More specifically, can integrins activate Syk via a similar conformational mechanism as pITAM? Are other integrin-associated kinases required for the activation? Here we used *in vitro* kinetic fluorescence-based assay to study the effect of the integrin β_3 cytoplasmic domain peptide on the activity of Syk. Our results show that soluble integrin peptides do not directly activate Syk as pITAM peptide does. On the other hand, we show that clustered integrin peptides can induce Syk activation independently of other kinases, presumably via an auto/transphosphorylation mechanism.

Results

Syk activity measurement using real-time fluorescence-based assay

To study the regulation of Syk *in vitro*, we first characterized the enzymatic properties of our purified full-length Syk protein (Fig. 1). To monitor kinase activity, we used a substrate peptide with SOX fluorophore ((S)-2-amino-N^{α}-(9-fluorenylmethyl-oxycarbonyl)-3-[8-hydroxy-5-(N,N-dimethylsulfonamido) quinoline-2-yl]propionic acid), whose fluorescence is modulated by phosphorylation (13, 25–27). As shown before (14), purified full-length Syk has low initial activity, which is enhanced in the presence of ATP after a lag period (Fig. 2A). This indicates that Syk has an intrinsic autophosphorylation or transphosphorylation activity that can initiate protein activation by phosphorylation of specific tyrosines residues along the structure (14). Because calculation of initial reaction velocity v_i is meaningless for the inactive or partially active enzyme, we analyzed the kinetic parameters of the activated Syk that was first incubated for 30 min with ATP (Fig. 2, *B–D*). The data were fitted to the ternary model equation because it has been previously shown that Syk kinase substrate binding fits better with ternary complex equation instead of the ping-pong model (28). K_m for SOX peptide was estimated to be 6 ± 1 μM and K_m for ATP was 29 ± 3 μM. The k_{cat}, calculated considering the initial velocity, was 22 ± 3 min^{-1}.

Syk can be activated by pITAM but not by soluble integrin β_3 tails

The interaction between the integrin cytoplasmic tail and Syk is mediated by tSH2 (22). We used surface plasmon resonance (SPR) to confirm the interaction between tSH2 and the integrin β_3 cytoplasmic tail peptide. The integrin peptide was coupled on the surface and increasing concentrations of tSH2 were injected on the sensor. The interaction had a fast, concentration-dependent association phase and concentration-independent dissociation phase (Fig. 3A). When the experimental data were fitted with Langmuir equation, the kinetic parameters were: $k_{on} = 398 \pm 87$ M^{-1} s^{-1}, $k_{off} = (3.22 \pm 0.12) \, 10^{-3}$ s^{-1}, and $K_D = (8.1 \pm 1.5) \, 10^{-6}$ M. Because the association phase was very fast and the Langmuir model is mainly based on the equilibrium levels, we also calculated the kinetic parameters assuming a single binding site and using the association and dissociation data only (Fig. 3, *B–E*) (see "Experimental procedures") (29, 30). With this method, the calculated kinetic parameters were: $k_{on} = 604 \pm 212$ M^{-1} s^{-1}, $k_{off} = (2.68 \pm 0.20) \, 10^{-3}$ s^{-1}, and $K_D = (4.44 \pm 1.55) \, 10^{-6}$ M. As expected, the k_{off} values were comparable, whereas the k_{on} calculated with the Langmuir model is half of the one calculated using first-rate reaction equation. We reason that the kinetic model should in this case be more accurate. On the other hand, the calculated K_D are comparable. Thus we consider that the K_D value of 4.44 ± 1.55 μM is the best estimate from our data.

With β_3 integrin/Syk interaction parameters in hand, we next compared the effect of saturating concentrations of pITAM and β_3 integrin tail peptides on Syk activity. As expected, 10 μM pITAM significantly reduced the lag phase on Syk activation. However, 30 μM β_3 tail peptide failed to do so (Fig. 4A). When both peptides were present, the integrin peptide did not change the effect of pITAM. When active Syk was used in this assay in the presence of a saturating concentration of SOX peptide neither pITAM nor integrin showed any effect (Fig. 4B).

To further analyze the effect of integrin β_3 cytoplasmic tail, we investigated the possible activity modulation of active Syk.
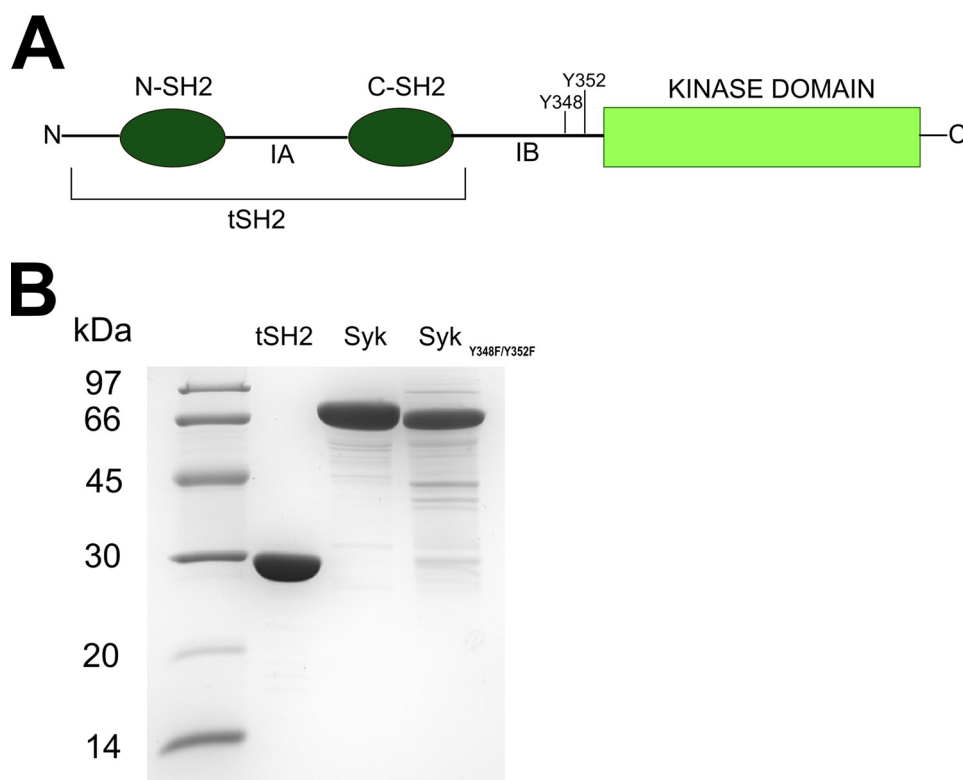
Figure 1. *A*, schematic representation of the Syk kinase structure. The N-SH2 and C-SH2 are the regulatory domains that are connected to each other through IA; they are named tandem SH2 (*tSH2*) together. tSH2 are connected to kinase domain via IB. Tyrosines 348 and 352 get phosphorylated during protein activation and in this study were mutated to phenylalanine. *B*, SDS-PAGE of purified proteins. For each protein preparation 5 μg of protein was loaded on the gel.

To assess the integrin effect on K_m for the SOX peptide, the ATP concentration was kept in saturating concentration and different concentrations of SOX peptide ranging from 1.5 to 30 μM were tested in the presence of integrin peptide (from 0 to 100 μM). The same experiment was done to test the effect of integrin on K_m for ATP: SOX peptide was in saturating concentration and ATP was tested from 10 to 100 μM. The double-reciprocal plots (Fig. 4, *C* and *D*) are consistent with integrin being a weak competitive inhibitor for the SOX peptide and non-competitive inhibitor for ATP. However, the inhibition was only observed at high integrin concentrations and the K_i values could not be accurately calculated, possibly due to poor solubility of the integrin peptide at 100 μM concentration. This is all consistent with the integrin peptide containing two tyrosine residues and being able to act as a substrate at high concentrations even though both tyrosines are not preceded by negatively charged amino acids that are required for good Syk substrates (31). Taken together, these data show that the integrin β_3 tail peptide does not directly activate Syk, but it may be a substrate or competitive inhibitor at high concentrations.

Clustered integrin β_3 tails can enhance Syk activation

In contrast to our *in vitro* findings, assays with platelets or cultured cells have shown that integrin ligation enhances Syk activity (21, 25). This could either be mediated by other kinases activated by integrin, such as Src family kinases, or by integrin clustering. To mimic integrin clustering *in vitro*, integrin β_3 peptide was coupled through the thiol group of the N-terminal cys-

teine on the assay plate at a high concentration. The clustered integrin peptide caused a significant reduction of the lag phase of Syk activity (Fig. 5A). Moreover, this effect was additive to that of the soluble pITAM peptide. This is consistent with the hypothesis that recruitment of Syk to integrin clusters will enhance its transphosphorylation and thus lead to increased local activity of the enzyme. As expected, clustered integrin did not have any effect on the pre-activated Syk (Fig. 5B).

Syk mutant (Y348F/Y352F) can be activated by clustered integrin β_3 tails

There are two tyrosine residues in the linker peptide of C-SH2 and the kinase domain Syk (Tyr-348 and Tyr-353 in human and Tyr-342 and Tyr-346 in mouse) that have been reported to be the main phosphorylation sites required for activation of Syk via Src-family kinases (Fig. 1). To find out if these residues are required for integrin clustering-induced activation of Syk, we studied the activation of double mutant Syk (Y348F/Y352F). Consistently with literature (13), this mutant has a low basal activity that can be enhanced by the pITAM peptide (Fig. 6A). Surprisingly, Syk (Y348F/Y352F) activation was enhanced by the clustered integrin in a similar way as that of wildtype Syk. This suggests that Syk clustering by integrins causes transphosphorylation of Syk activation tyrosine residues other than Tyr-348 and Tyr-352.

Discussion

Syk plays a crucial role in diverse types of cells and it is involved in many biological processes. In this paper we have
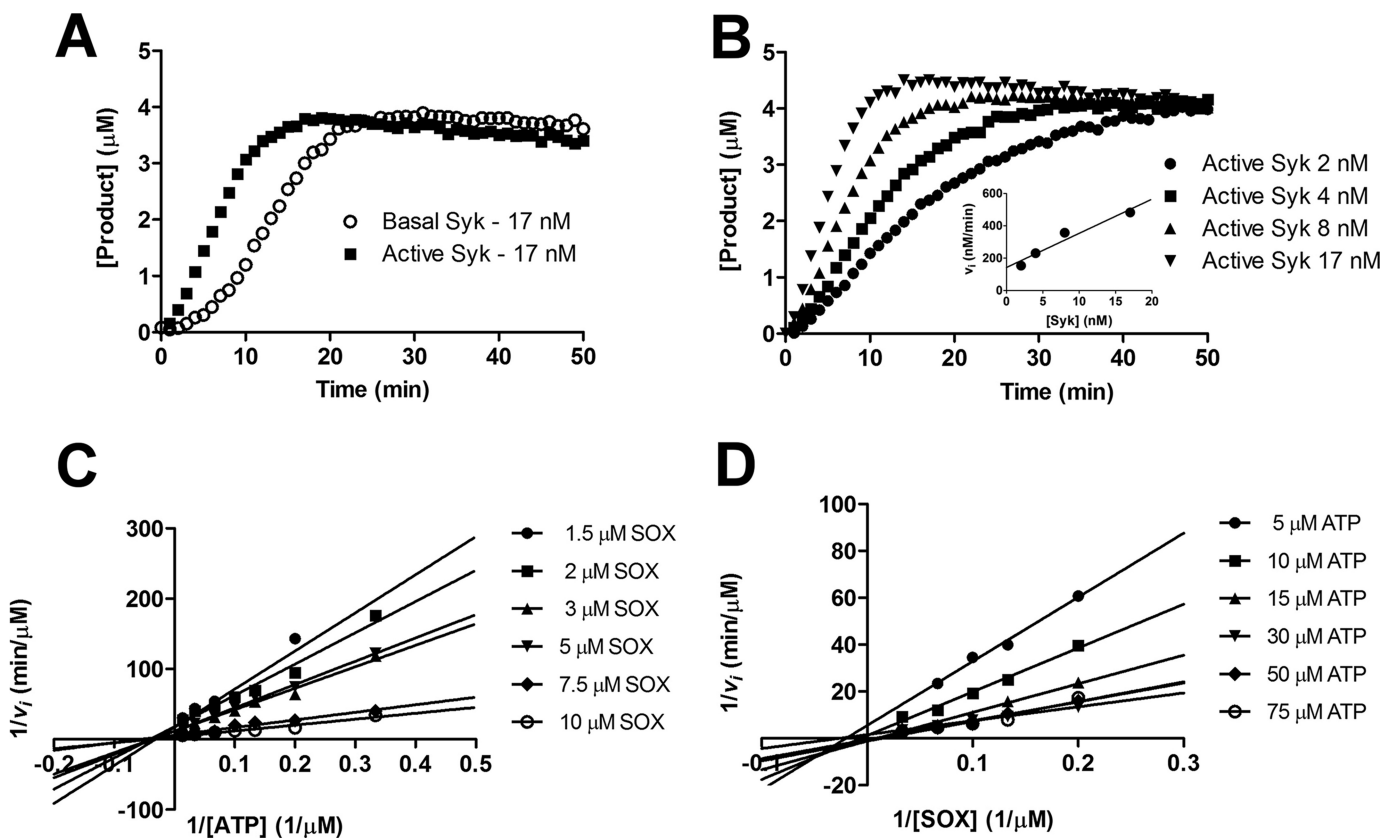
Figure 2. Kinetic characterization of Syk kinase. *A*, time course (min) of SOX peptide phosphorylation (μM) for basal Syk (*open circles*) and active Syk (*squares*). Syk was activated through incubation with 100 μM ATP for 30 min at room temperature. Basal Syk and active Syk were used at the same concentration of 17 nM; basal Syk showed a ~5 min lag phase, which was abolished in the active Sky. *B*, kinetic measurements of active Syk at different concentrations (2, 4, 8, and 17 nM). The *inset* shows the initial reaction speed (nM/min) calculated using linear regression fit from 5 to 15 min plotted against the active Syk concentration (nM). The calculated k_{cat} in this experiment was 22 ± 3 min^{-1}. *C* and *D*, Lineweaver-Burk plot generated from two-substrate analysis measurements of $1/v_i$ versus $1/[\text{ATP}]$ (*C*) and $1/[\text{SOX}]$ (*D*). Experimental data were fit with a ternary complex equation and the calculated K_m was 6 ± 1 μM for SOX peptide and 29 ± 3 μM for ATP.

studied the consequences of integrin cytoplasmic domain binding to the enzymatic activity of Syk. Although it is well established that pITAM containing receptors induce conformational changes in the regulatory domain of Syk and thus cause direct activation of the kinase domain, it has not been studied before whether integrin cytoplasmic domain peptides binding to the same region as pITAM can do the same. We found that soluble integrin peptides were not able to induce direct activation of Syk. Instead, integrin clustering could induce autophosphorylation of Syk and thus enhance its activation. These two main findings are discussed below.

There are two pathways for the initialization of Syk activation. This property has been named the OR gate switch model of Syk activation (15) meaning that Syk activation can either be initialized via pITAM binding to tSH2 or via phosphorylation. The molecular details of the pITAM/tSH2 interaction are known (32). Briefly, the N-SH2 interacts with the C-terminal pY*XX*L/I motif in ITAM receptor and the C-SH2 with the N-terminal pY*XX*L/I motif. The structures of two SH2s are very similar and they contain a positively charged pocket to accept the phosphotyrosine and a hydrophobic pocket to accommodate the leucine/isoleucine. It seems that for pITAM binding both SH2s are needed even if the C-SH2 seems to be more flexible and unstable compared with N-SH2 (32). As a consequence of pITAM binding, the orientation of tSH2 in relation-

ship to the kinase domain changes and this releases the hinge between two globes of the kinase leading to enhanced activity. The other arm of the OR gate switch model implies that at least Tyr-348, Tyr-352, and Tyr-630 can be phosphorylated directly by Src family kinases such as Lyn, or auto/transphosphorylated by Syk itself. This can also lead to full activation of the enzyme independent of the interaction with pITAM (15).

Here our aim was to relate the OR gate switch model to integrin-mediated Syk activation. Syk interacts with integrins through tSH2 and, specifically, the N-SH2 and IA are mostly involved, whereas the C-SH2 has a marginal contribution (22). We confirmed the interaction between isolated tSH2 and integrin β_3 cytoplasmic tail using SPR experiments; the measured K_D was 4.44 ± 1.55 μM, which indicates a medium-low affinity binding. Woodside *et al.* (22) reported a higher affinity (K_D 24 nM) using different peptides and different Syk preparations. This discrepancy in the determined affinities should not affect our enzyme activation assays as we used 30 μM concentration of integrin peptide, which should be close to saturating concentration. We found that soluble integrin cytoplasmic domain peptides did not change the lag phase of Syk activation in the same way as pITAM peptides. Furthermore, integrin did not inhibit pITAM-induced activation. This is consistent with pITAM and integrins having distinct binding sites (21, 22). Our
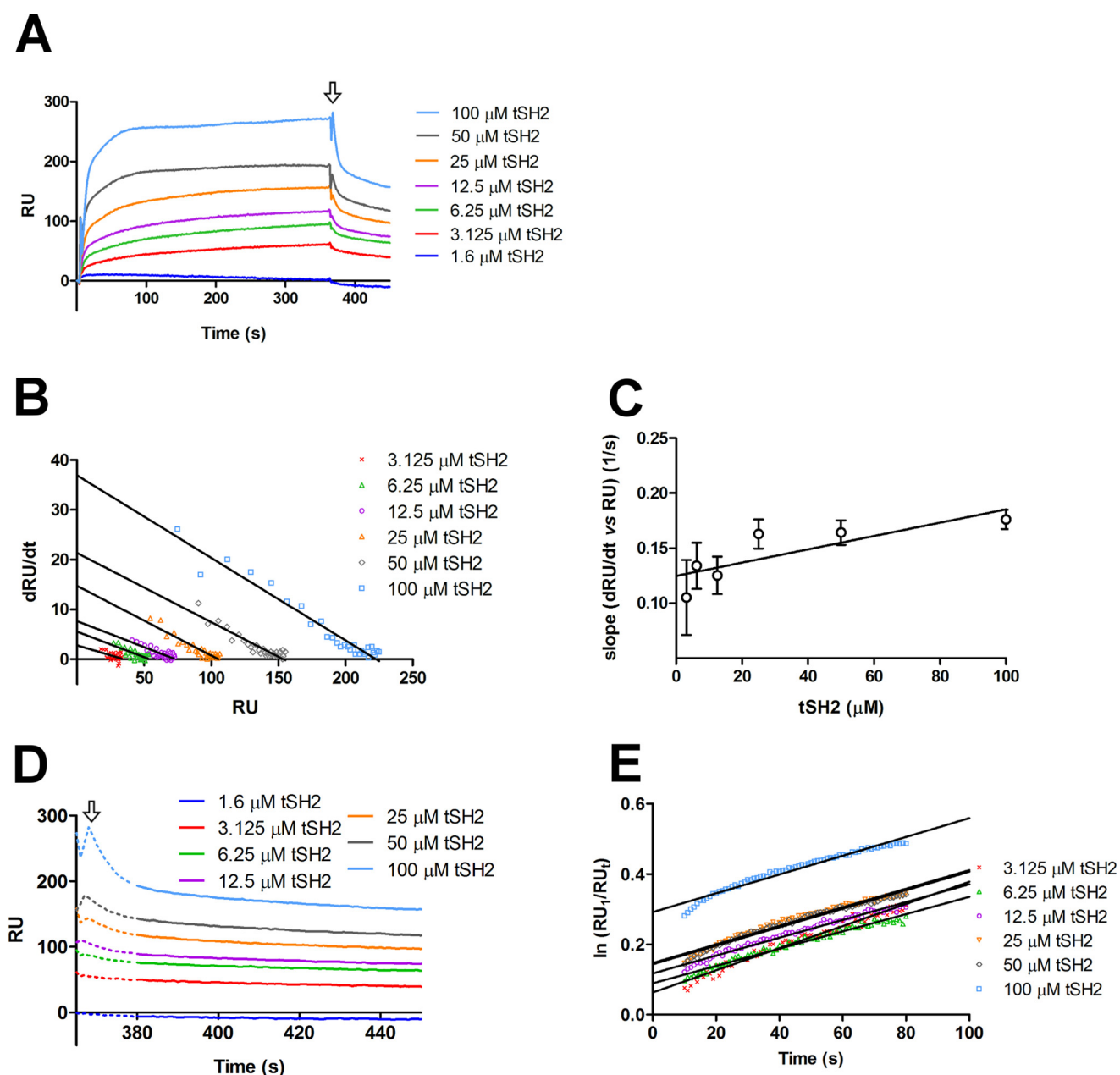
Figure 3. Interaction between tSH2 and integrin β_3 tail. *A*, SPR experiment where integrin β_3 tail peptide was coupled on the surface (ligand) and different concentrations of tSH2 (from 1.3 to 100 μM) were injected (analyte). In the graph is plotted the variation of the RU in the time (s) for each tSH2 concentration tested. The *arrow* indicates the stop of the injection and, therefore, the beginning of the dissociation phase. *B*, dRU/dt (variation of RU in time) is plotted against RU (from 10 to 30 s of the association curve, see *panel A*). *Solid lines* correspond to the best linear regressions calculated for each tSH2 concentration. *C*, calculation of association rate constant (k_{on}) of the tSH2–integrin β_3 tail peptide complex formation. *Error bars* are derived from linear regression analysis of *panel B* in this figure (see "Experimental procedures"). *D*, variation of RU in the time (s) of the dissociation phase. The *arrow* indicates the end of injection as in *panel A*. The *dotted line* corresponds to the part of dissociation curve that was not used for the determination of the dissociation rate constant (see *panel E*), whereas the *solid line* indicates the part that was used. *E*, variation of $\ln(RU_1/RU_t)$ in time (s), the best linear fits are represented with *solid lines*. RU_1 indicates the response units at the beginning of dissociation phase, and RU_t indicates the response units at the time t. The slope of the linear regression corresponds to the dissociation rate constant (k_{off}) (see "Experimental procedures").

results thus indicate that integrins do not induce similar conformational changes in tSH2 as pITAM.

We also performed competition experiments using the β_3 integrin cytoplasmic domain peptide with the active Syk kinase and its ATP substrates and the SOX peptide. In this assay integrin β_3 peptide acted as a competitive inhibitor toward the SOX peptide and showed characteristics of uncompetitive inhibition toward the ATP. In both cases the inhibition was observed at considerably higher concentrations than the

measured K_D for the integrin binding to the tSH2 of Syk. Due to technical problems related to low inhibitory activity, we were not able to calculate K_i values using these data. The simplest explanation of the observed effect is that the tyrosine-containing sequences in the integrin peptide can compete with the substrate peptide. Similar behavior has been observed earlier with ITAM peptides: even though they do not contain the optimal Syk substrate recognition sequences, at high concentrations they reduce Syk activity
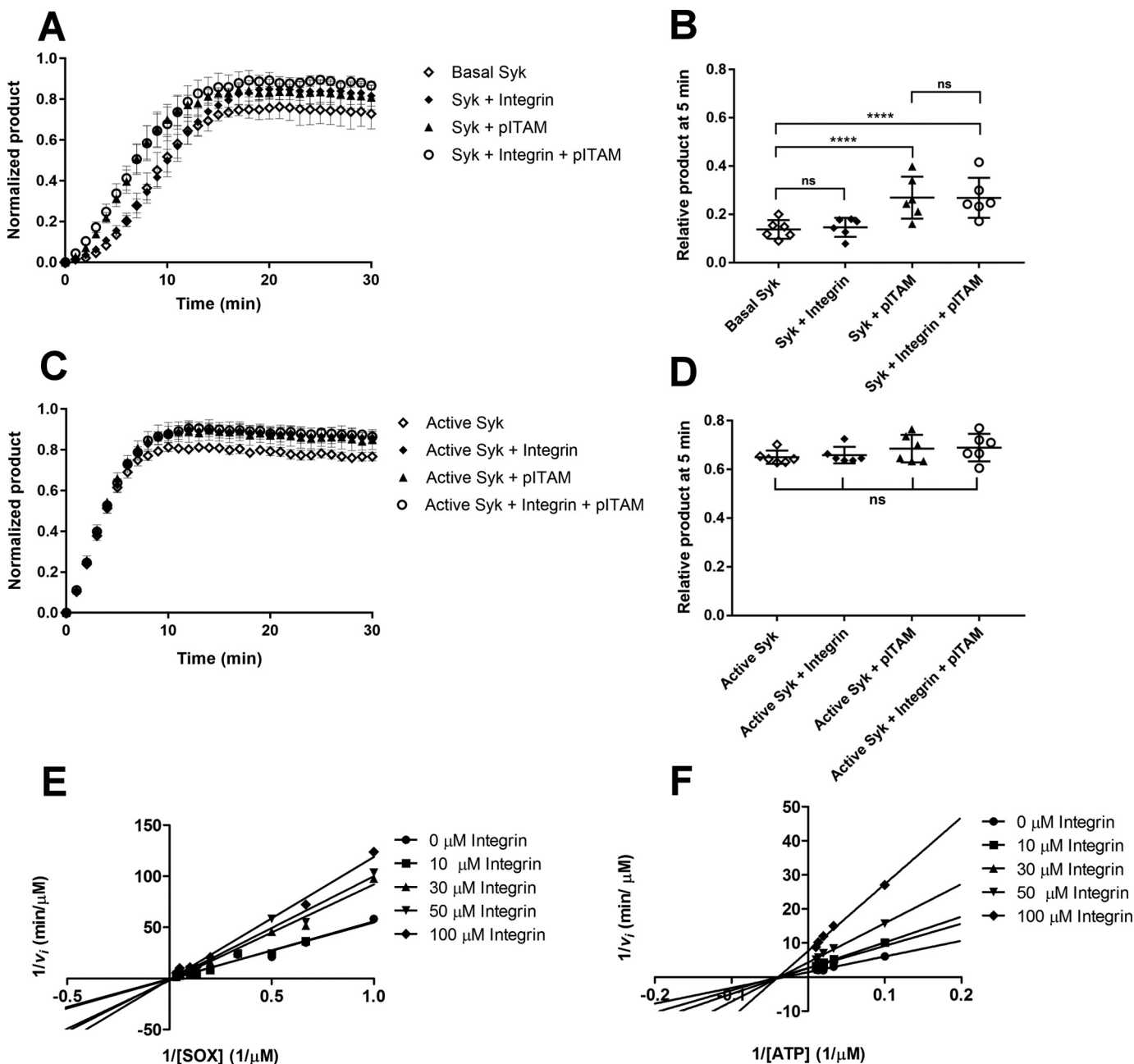
Figure 4. Effect of pITAM and integrin β_3 tail on Syk wildtype activity. *A,* kinetic measurement of Basal Syk in the absence of peptide (*open diamonds*), in presence of 30 μM integrin β_3 cytoplasmic tail peptide (*diamonds*), 10 μM pITAM peptide (*triangles*), and a combination of both (*open circles*). The activity is expressed in terms of normalized product formation in time (min); basal Syk was used at concentration of 17 nM. *Error bars* correspond to the standard deviation calculated from six different experiments. *B,* ANOVA of the 5-min time point in the experiment shown in *panel A*. The data indicate that the presence of soluble pITAM activates the protein reducing the lag-phase of basal Syk. *p* value for basal Syk *versus* Syk + pITAM and basal Syk *versus* Syk + pITAM + integrin were both <0.0001. Comparing the basal Syk *versus* Syk + integrin and the Syk + pITAM *versus* Syk + integrin + pITAM with the ANOVA test resulted in nonsignificant (*ns*) *p* values thus showing that the soluble integrin β_3 cytoplasmic tail peptide had no effect. *C,* kinetic measurement of active Syk in the absence of peptide (*open diamonds*), in the presence of 30 μM integrin β_3 cytoplasmic tail peptide (*diamonds*), 10 μM pITAM peptide (*triangles*), and a combination of both (*open circles*). The activity is expressed in terms of normalized product formation in time (min). Active Syk was used at 17 nM. *D,* the ANOVA of the 5-min time point in *panel C*; it resulted in a nonsignificant (*ns*) *p* value suggesting that the pre-activated Syk is not modulated by the presence of either of two peptides. *E* and *F,* Lineweaver-Burk plots showing the competitive inhibition toward SOX peptide (*E*) and uncompetitive inhibition toward ATP (*F*) by the integrin β_3 cytoplasmic tail. In each case $1/v_i$ was plotted against 1/[SOX] (*E*) or 1/[ATP] (*F*). The experiments were carried out using active Syk at 4 nM.

(14). Whether this phenomenon has any relevance to physiological Syk function, remains unclear.

To study the possible contribution of integrin binding to the other arm of the OR gate switch model, we mimicked integrin clustering *in vitro* by coupling the β_3 cytoplasmic domain peptide via its N terminus to the surface of the enzymatic assay plate. Integrin clustering is the basis of many, if not all, integrin adhesion-induced signaling events (33). Integrin clustering is partly mediated by extracellular ligands, partly by adhesome components such as talin and kindlin, and partly by actin cytoskeleton (34). Integrin clusters are dynamic structures where several components are exchanged rapidly (34, 35). We found
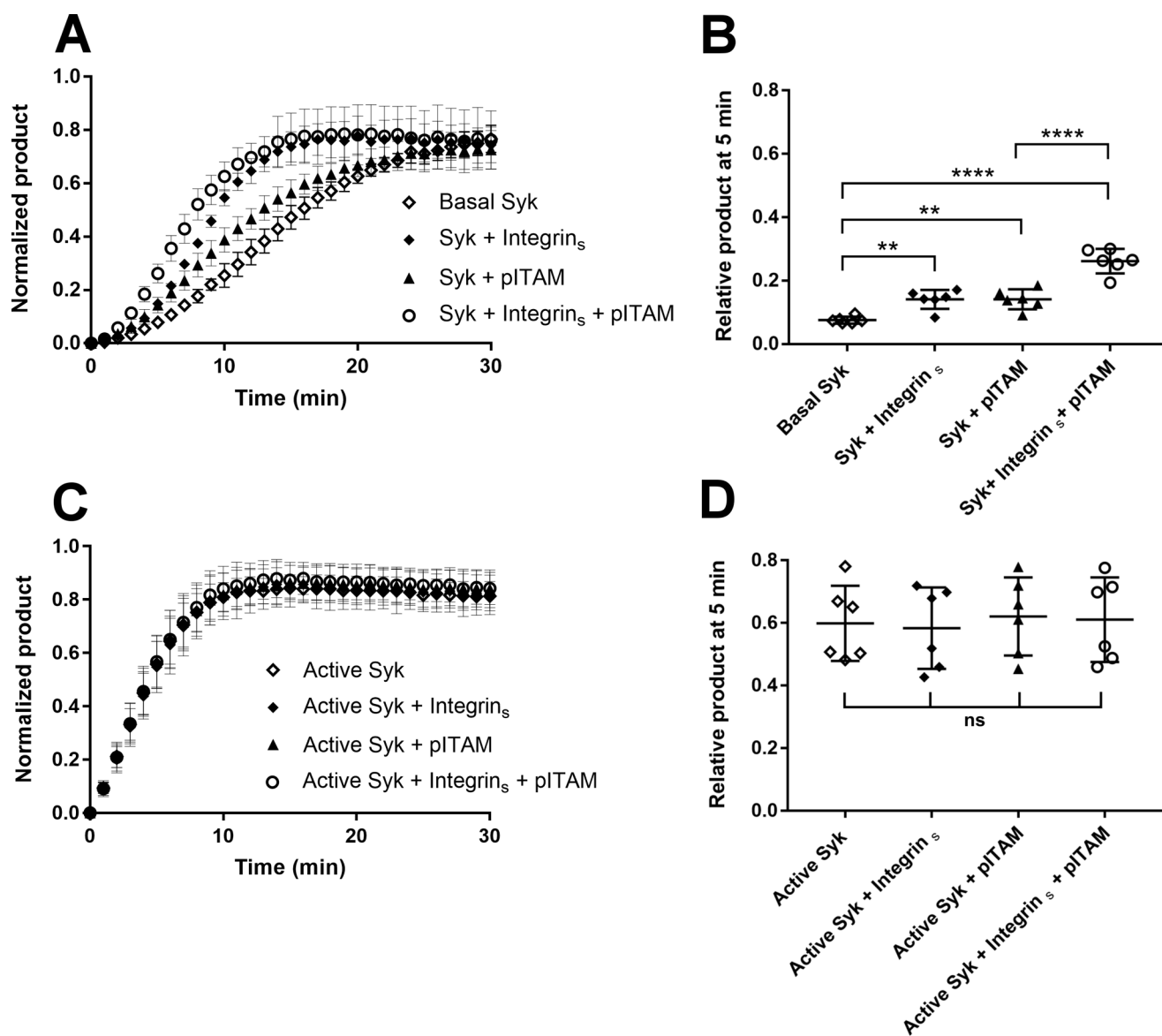
Figure 5. Effect of clustered integrin β_3 cytoplasmic tails on Syk activation. *A,* time course (min) of the normalized product formation in the absence of peptides (*open diamonds*) and in the presence of the integrin β_3 cytoplasmic tail peptide coupled on the assay plate surface (*diamonds*), 10 μM pITAM (*triangles*), and combination of the two peptides (*open circles*). Basal Syk was used at 17 nM. *Error bars* correspond to the standard deviation calculated using six different experiments. *B,* ANOVA of the 5-min time point in *panel A*. The experiment shows that surface-bound integrin peptide reduces the lag phase of basal Syk; *p* value for basal Syk *versus* Syk + integrin$_s$ was 0.0014 and was comparable with the *p* value for basal Syk *versus* Syk + pITAM, which was 0.0013. A combination of two peptides further accelerated the process (*p* value <0.0001). Integrin β_3 cytoplasmic tail bound on the plate surface also has a synergic effect in the presence of pITAM peptide, in fact comparing the Syk + pITAM *versus* Syk + pITAM + integrin$_s$ the ANOVA test gave a *p* value <0.0001. *C,* time course (min) of the normalized product formation in the absence of peptides (*open diamonds*) and presence of the integrin β_3 cytoplasmic tail peptide coupled on the assay plate surface (*diamonds*), 10 μM pITAM (*triangles*), and a combination of two peptides (*open circles*). Active Syk was used at 17 nM. *D,* ANOVA of the experiment shown in *panel C*. *p* values were calculated using a ANOVA test including six separate experiments using the relative product formed at the 5-min time point as described under "Experimental procedures." *p* values were nonsignificant (*ns*).

that clustered integrin peptides significantly reduced the lag phase of Syk autoactivation. This effect was additive with the pITAM-induced activation. We take this as evidence that integrin clustering rapidly induces Syk transphosphorylation by bringing several kinase molecules in close proximity, leading to increased local concentration (Fig. 7). We also found that the Syk (Y438F/Y352F) mutant could be activated by clustered integrins. This shows that in addition to the main regulatory tyrosines 348 and 352, there are other residues that can be transphosphorylated by the Syk itself and that activate the

kinase. Although it has been shown that activation loop tyrosines 525 and 526 have little effect on Syk activity, it is well established that the C-terminal tyrosines 630 and 631 can stabilize the closed, inactive conformation of the enzyme (13, 36), and thus phosphorylation of these could induce the activity of even the Y438F/Y352F mutant. In mouse, Syk residues corresponding to Tyr-630 and Tyr-631 have been found to be autophosphorylated or transphosphorylated (37).

In conclusion, enzyme kinetic studies presented here imply that integrin cytoplasmic domain peptides do not
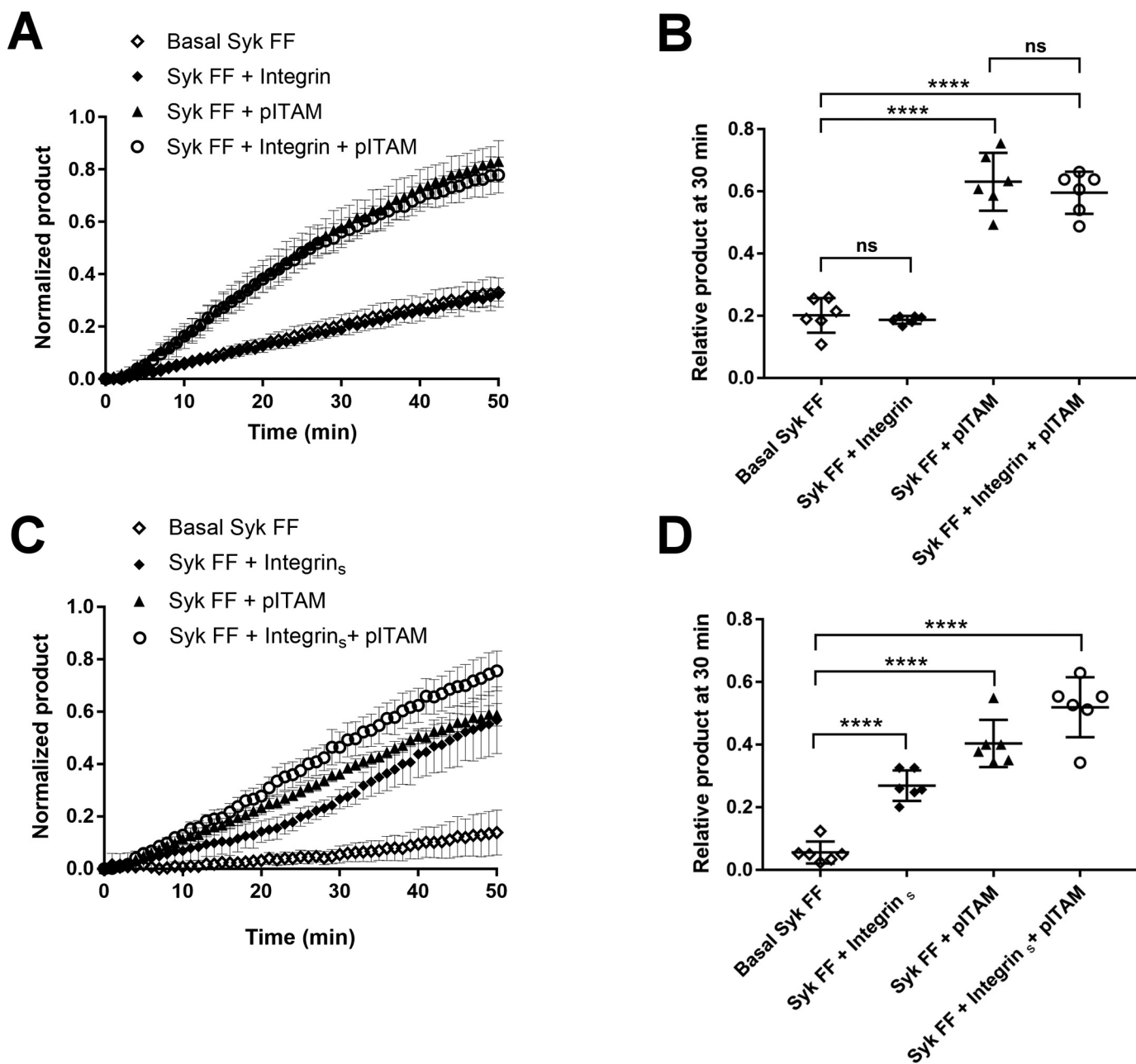
Figure 6. Effect of pITAM and clustered integrin β_3 tails on Syk Y348F/Y352F mutant activation. *A,* kinetic measurement of Syk mutant activity in the absence of peptides (*open diamonds*), 30 μM integrin β_3 tail peptide (*diamonds*), 10 μM pITAM (*triangles*), and a combination of both peptides (*open circles*). Syk FF was used at 17 nM concentration and the *error bars* are derived from the calculated standard deviation from six different experiments. *B,* ANOVA of the 30-min time point in *panel A*. Comparison of basal Syk FF *versus* Syk FF + integrin and the Syk FF + pITAM *versus* Syk FF + integrin + pITAM revealed that the soluble integrin peptide does not activate Syk FF (*p* value non-significant, *ns*) in contrast to pITAM (*p* values <0.0001). *C,* the same experiment described in *panel A*, except the integrin β_3 tail peptide, which was coupled on the plate surface. *D,* ANOVA of the 30-min time point in *panel C*. All *p* values were <0.0001.

induce direct conformational changes in Syk and do not lead to its activation with a similar mechanism as pITAM. Instead, we propose that integrin clusters may increase the local concentration of Syk and enhance its activity via increased transphosphorylation.

Experimental procedures

Syk full-length expression and purification

Spleen tyrosine kinase (*SYK*) (EC 2.7.10.2) sequence cDNA (UniProt ID: P43405) was obtained from Origene Technologies Inc. (Rockville, MD) and a fragment containing amino acids 1–635 was expressed with the cleavable N-terminal His$_6$ tag (MSGSHHHHHHGSSGENLYFQ $\downarrow$ SL, where $\downarrow$ denotes a tobacco etch virus (TEV) cleavage site) with pFastBac NT-TOPO (Bac-To-Bac expression system, Invitrogen, Thermo Fisher Scientific Inc.). The sequence of the expression expression construct was verified by Sanger sequencing. *Spodoptera frugiperd*a (Sf9) insect cells were transfected using Cellfectin II reagent (Thermo Fisher Scientific Inc.) using the manufacturer's protocol. Recombinant protein
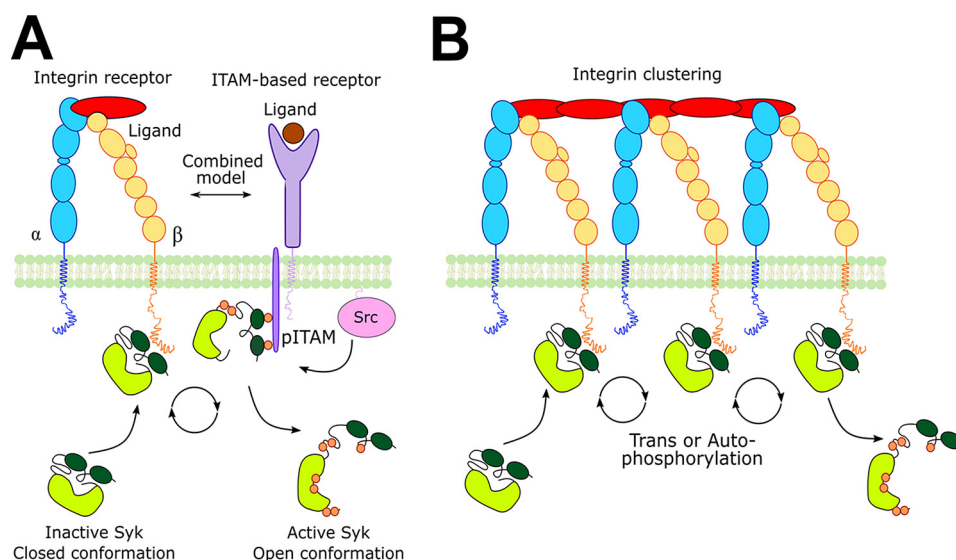
Figure 7. A model of Syk activation mediated by clustered integrins. Integrin receptor subunits α and β are represented in *blue* and *yellow*, respectively. ITAM containing receptor is in *purple*. Src family kinase is represented in *pink*; Lyn kinase is the Src kinase, which is mainly involved in the Syk activation procedure. Syk is represented in two conformations (*closed* and *open*). The kinase domain is *light green*, whereas the SH2 domains are in *dark green*, *black lines* indicate the linker regions. The *small orange circles* represent the phosphorylations along the Syk structure. *A*, combined model of Syk activation mediated by integrin and ITAM-containing receptors. Syk is recruited near the membrane by the interaction with integrin tail and phosphorylated ITAM. Syk is first activated by interaction with pITAM through conformational rearrangement in the kinase structure. Then it can be phosphorylated by other kinases recruited via the integrin pathway. Src-family kinases may be responsible for the phosphorylation of both ITAM receptor and Syk. *B*, Syk activation model mediated by integrin clustering. Inactive Syk can interact with the integrin tail. The proximity effect enhances Syk trans/autophosphorylation activity leading to Syk activation. Importantly, this pathway can occur independently of pITAM and Src family kinases.

was expressed as described previously (38). Cells were harvested 72 h after infection (multiplicity of infection = 1) by centrifugation at $500 \times g$ and resuspended in cold lysis buffer (50 mM sodium phosphate, 500 mM NaCl, 5 mM MgCl$_2$, 0.1% Nonidet P-40, 1 mM dithiothreitol (DTT), pH 8); Pierce™ Universal Nuclease for Cell lysis (ThermoFisher) 25 units/ml and protease inhibitors tablet (cOmplete™ Protease Inhibitor mixture, Sigma) were added separately to resuspended cells. 5 ml of lysis buffer was used for grams of wet mass. Cells were sonicated (10 times, 1-s pulse) in ice, and then the cells suspension was clarified by centrifugation at $100,000 \times g$ for 1 h, 4 °C. Supernatant was loaded on a pre-equilibrated (50 mM sodium phosphate, 500 mM NaCl, 10 mM imidazole, pH 8) His Trap FF, 1-ml prepacked column (GE Heathcare Inc.) with peristaltic pump at a flow rate of 0.5 ml/min, 4 °C. The column was washed with binding buffer and protein was eluted by stepwise imidazole gradient (10, 20, 50, 100, 250, and 500 mM imidazole in 50 mM sodium phosphate, 500 mM NaCl, pH 8). Fractions containing Syk were pooled and concentrated using Amicon® Ultra 15-ml Centrifugal Filter, 30-kDa cutoff (Merck KGa). Protein was then loaded on HiLoad 10/30 Superdex 200 column (GE Heathcare Inc.) equilibrated with 10 mM Hepes, 150 mM NaCl, 10% glycerol, 10 mM methionine, 1 mM DTT, pH 7.5. Protein was concentrated to final concentration of 2 mg/ml; aliquots were frozen in liquid nitrogen and stored in -80 °C.

Syk mutant (Y348F/Y352F) was obtained with a QuikChange Multi-Site-directed Mutagenesis Kit (Agilent Technologies Inc.) using wildtype Syk as template. Sf9 insect cells were harvested after 48 h infection (multiplicity of infection = 3) and lysed as described for Syk wildtype. Protein was purified as the

wildtype except that the affinity purified protein was incubated with TEV overnight at 4 °C to remove the His$_6$ tag. Protein was then concentrated and loaded for gel filtration as described for Syk wildtype. The final protein preparation was concentrated to 1 mg/ml. The final protein sequence contains the Leu–Ser sequence remaining from the TEV recognition site.

Tandem SH2 domains expression and purification

Tandem SH2 (amino acids 9–264) was cloned in plasmid pGTvL1-SGC (Structural Genomics Consortium, University of Oxford) using a ligation-independent method (39). The final construct was sequence verified. The final protein sequence contains a Ser–Met sequence that remained from the vector. tSH2 were expressed using *Escherichia coli* BL21 gold cells (Agilent Technologies Inc.) at 30 °C for 4 h with 0.4 mM isopropyl β-D-1-thiogalactopyranoside. The bacterial pellet was lysed using a French press. The protein was captured with on a glutathione-agarose column (Protino glutathione-agarose 4B, Macherey-Nagel Gmbh) equilibrated with 20 mM Tris, 100 mM NaCl, 1 mM DTT, pH 8, and then eluted using same buffer containing 50 mM glutathione. Glutathione *S*-transferase–tSH2 complex was cut using TEV protease (Invitrogen), and further purified by size exclusion chromatography with a HiLoad 26/60 Superdex 75 column (GE Healthcare) in 20 mM Tris, 100 mM NaCl, 1 mM DTT, pH 8. The final protein preparation was concentrated using a Amicon® Ultra Centrifugal Filter, 30-kDa cut off to 30 mg/ml. Aliquots were frozen in liquid nitrogen and stored at -80 °C.

MS data acquisition and processing

Purified proteins were analyzed by mass spectrometry using a Q-TOF type instrument (Waters Synapt G1) connected to an

Acquity (Waters) UPLC chromatography system equipped with a C4 reversed phase column (Waters BEH300 C4 1.7 μm, 2.1 × 100 mm). Protein samples were diluted 10-fold with 0.1% trifluoroacetic acid (TFA) and 3-μl aliquots were injected. The eluents were 0.1% formic acid in water (A) and 0.1% formic acid in acetonitrile (B). The gradient was from 3 to 60% B over 8 min. The mass spectrometer was tuned for detection of proteins to take 1-s lock mass (Leu encephalin) corrected scans in the mass range from 500 to 2000 m/z. Combined mass spectra for the chromatographic peaks were deconvoluted using the MaxEnt 1 algorithm as part of Masslynx (Waters). For tSH2 the measured molecular mass was 29,160 Da (expected 29,163 Da), for Syk WT it was 74,443 Da (expected: 74,525 Da), and for Syk FF it was 72,230 Da (expected 72,234 Da).

Surface plasmon resonance

The SPR experiment was done using a Biacore X instrument (GE Healthcare Inc.). Integrin β_3 cytoplasmic tail peptide (UniProt ID: P05106 CKFEEERARAKWDTANNPLYKEATSTFT-NITYRGT, ProteoGenix, Schiltigheim, France) was coupled onto CM5 (GE Healthcare) chips using thiol coupling. The immobilization step was done at a 5 μl/min flow rate with a single flow cell. The carboxymethyl–dextran surface was activated using 1:1 ratio of 0.4 M 1-ethyl-3-(3-dimethylaminopropyl)carbodiimide and 0.1 M N-hydroxysuccinimide for 10 min. Then, 0.1 M ethylenediamine, 0.1 M sodium borate, pH 8.5, for 7 min, and 1 M ethanolamine, pH 7, for 10 min were injected. To introduce thiol-reacting groups the surface was coupled with 50 mM Sulfo-GMBS (N-[γ-maleimidobutyryloxy]succinimide) in 0.1 M sodium borate, pH 8.5, for 4 min. The peptide was diluted using 10 mM Hepes, pH 7, at 50 μg/ml and injected for 10 min to maximize the reactivity with sulfo-GMBS. Finally, the surface was blocked with 50 mM cysteine, 1 M NaCl, 0.1 M sodium acetate, pH 4, for 4 min. The experiment with tSH2 was carried out with 10 mM Hepes, 150 mM NaCl, pH 7.5, as running buffer and the flow rate of 10 μl/min using two flow cells. 2-Fold dilutions of tSH2 were prepared in the running buffer starting from 1.6 to 100 μM. Each sample was injected for 6 min with a delayed wash of 150 s. No surface regeneration was done between injections. Each measurement was done at least three times using different chips. The final resonance units (RU) were obtained by subtracting the binding response obtained with the nonfunctionalized sensor from that obtained from the integrin β_3 cytoplasmic tail peptide-coupled cell. The original response curves were fit using a Langmuir model with Biacore evaluation software 3.1 provided by the manufacturer. The data were then analyzed following the method previously described (29, 30). Briefly, to calculate the association rate k_{on} of complex integrin peptide–tSH2 the data from 10 to 30 s after injection were used. First a plot of dRU/dt (variation of RU in time) *versus* RU was done, and then the slopes obtained from linear regressions were replotted against the tSH2 concentrations used. The k_{on} is calculated based on equation,

$$\text{Slope}\left(\frac{d\text{RU}}{dt} vs \text{RU}\right) = k_{on} \times C + k_{off} \qquad \text{(Eq. 1)}$$

where k_{on} is the association constant, C is the protein concen-

tration injected, and k_{off} is an estimation of the dissociation rate of the complex. Because the dissociation rate is not dependent on protein concentration it can be obtained using a first-rate reaction equation,

$$\ln\left(\frac{R_1}{R_t}\right) = k_{off} \times t \qquad \text{(Eq. 2)}$$

where R_1 is the RU at the end of sample injection, R_t is the RU at the time t, and k_{off} is the dissociation constant. The K_d is equal to k_{off}/k_{on}. Data analysis was performed using linear regression.

Fluorescence-based kinetic assay

Kinetic measurements of Syk were done using SOX fluorescent peptide (26, 27). The SOX peptide used was Ac-EEEEYIQ-[DPro-Sox-G]-NH$_2$ (Sigma) (28). The assay was performed in SOX assay buffer (20 mM Hepes, 0.1 mM EGTA, 1 mM MgCl$_2$, 10 μM sodium orthovanadate, 5 mg/ml of BSA, 1 mM DTT, pH 7.15) in a final volume of 50 μl. The fluorescence was detected with Victor$^{\text{TM}}$ X4 2030 Multilabel Reader (PerkinElmer Life Sciences) using 355 nm as excitation wavelength and 460 nm as emission wavelength in 96-well black plates at 30 °C. Data were collected every 30 s for at least 50 min. Each experiment was repeated six times and each measurement within an experiment was done in quadruplicate. Standard deviation was calculated using the data from six different experiments. Data were analyzed using repeated measurements one-way ANOVA (RM-ANOVA) followed by Tukey's multiple comparison test using GraphPad Prism 7. To conduct the ANOVA analysis data were first normalized to the highest measured product concentration in the presence of pITAM and integrin and then arcsine transformed.

Syk auto/transphosphorylation

Syk autophosphorylation was performed as previously described with some modifications (14). Syk wildtype, 2.7 μM, was incubated for 30 min at room temperature in the presence 100 μM ATP, in a buffer containing 15 mM Hepes, 20 mM NaCl, 10 mM MgCl$_2$, 1 mM EGTA, 10 μM sodium orthovanadate, 10% glycerol, pH 7.4, in a final volume of 2 ml. After incubation, excess ATP was washed away using a PD10 desalting column (GE Healthcare Inc.) using the same buffer and the protein was concentrated to 0.2 mg/ml with Amicon® Ultra Centrifugal Filter, 30 kDa cutoff.

Kinetic measurements of Syk activity and two-substrate analysis

Syk kinetic measurements were performed following the increase of the peptide fluorescence in the time as above described in the presence of 10 μM SOX peptide and 25 μM ATP. Basal Syk and active Syk were used at 17 nM, except for two substrate analysis where active kinase was used at 4 nM; the reaction was started by adding ATP as the last ingredient. Each measurement was done at least in triplicate; a blank without Syk was recorded also and it was subtracted from the fluorescence measured in the presence of the kinase. The two-substrate analysis was used to determine the K_m for ATP and the SOX peptide. Hence, in the case of K_m for ATP, the ATP concentration

was varied from 5 to 75 μM in the presence of a constant concentration of SOX peptide (from 1.5 to 30 μM). Likewise, K_m for SOX was determined changing the SOX peptide concentration from 1.5 to 10 μM in the presence of a constant concentration of ATP (from 5 to 75 μM). The data were analyzed assuming that the ternary complex model describes the Syk kinetic mechanism (28),

$$v = \frac{v_{max}[\text{ATP}][\text{SOX}]}{[\text{ATP}][\text{SOX}] + [\text{ATP}]K_m^{\text{SOX}} + [\text{SOX}]K_m^{\text{ATP}}K_a^{\text{ATP}}K_a^{\text{SOX}}} \quad \text{(Eq. 3)}$$

where K_m^{SOX} and $K_m^{\text{ATP}}{}_m$ are Michaelis–Menten constants of SOX and ATP, respectively, and K_a^{SOX} is the association constant of SOX for Syk.

K_m for ATP and SOX peptide were calculated using the following equations derived from Equation 3 assuming that one of the two substrates is kept in a constant concentration,

$$\frac{1}{v_{max(app)}} = \frac{K_{mSOX}}{V_{max}}\frac{1}{[\text{SOX}]} + \frac{1}{V_{max}} \quad \text{(Eq. 4)}$$

$$\frac{1}{v_{max(app)}} = \frac{K_{mATP}}{V_{max}}\frac{1}{[\text{ATP}]} + \frac{1}{V_{max}} \quad \text{(Eq. 5)}$$

where $V_{max(app)}$ corresponds to the apparent rate of the reaction in presence of a constant concentration of the other substrate.

Effect of pITAM and integrin β₃ cytoplasmic tail on kinase activation and on Syk activity

Basal and active Syk were tested in the presence of the pITAM peptide from the CD3ϵ chain (UniProt ID: P07766, NPDpYEPIRKGQRDLpYSGLNQR, ProteoGenix) and in the presence of the integrin β_3 cytoplasmic tail peptide. Both peptides were dissolved in water and added to the reaction mixture. The assay was performed as described above. pITAM peptide and integrin β_3 cytoplasmic tail peptide were used at concentrations of 10 and 30 μM, respectively; both basal and active Syk were 17 nM. Differently, the inhibition analysis was done using active Syk at 4 nM. Hence, to test the effect of the integrin β_3 cytoplasmic tail peptide on Syk affinity for the SOX peptide, the ATP concentration was kept constant to 250 μM (saturating concentration), SOX was varied from 1 and 30 μM, and the integrin peptide from 0 to 100 μM. Similarly, to assess the integrin peptide effect on Syk affinity for ATP, the SOX peptide concentration was kept constant equal to 30 μM (saturating concentration) and ATP concentration ranged from 10 and 100 μM.

Effect clustered integrin β₃ cytoplasmic tails on kinase activation

Integrin β_3 cytoplasmic tail peptide was coupled on the surface of the assay plate through thiol coupling. Pierce™ maleimide-activated plates (Thermo Scientific) were used for the coupling reaction following the methods suggested from the manufacturer with minor changes. The plate was first washed with washing buffer (0.1 M sodium phosphate, 0.15 M NaCl, pH 7.2); peptide was diluted with coupling buffer (0.1 M sodium phosphate, 0.15 M NaCl, 10 mM EGTA, pH 7.2) at 5 μM

and incubated for 2 h on a plate shaker. Then, the not-reacted groups were blocked with 10 μg/ml of cysteine·HCl in coupling buffer. Finally, the plate was washed and dried by centrifugation upside-down at $1000 \times g$. The SOX peptide-based assay was performed as described before except for the absence of DTT in the assay buffer.

Effect of pITAM and integrin β₃ cytoplasmic tail on Syk mutant (Y348F/Y352F)

To assess the effect of pITAM and integrin β_3 cytoplasmic tail peptide on Syk mutant activity, the same procedure described for Syk wildtype was used. Syk mutant was used at 17 nM and pITAM and integrin peptide at 10 and 30 μM, respectively. The same procedure was also used in the presence of the integrin β_3 cytoplasmic tail peptide coupled on the surface.

References

1. Yang, C., Yanagi, S., Wang, X., Sakai, K., Taniguchi, T., and Yamamura, H. (1994) Purification and characterization of a protein-tyrosine kinase p72^{syk} from porcine spleen. *Eur. J. Biochem.* **221,** 973–978 CrossRef Medline
2. Mócsai, A., Ruland, J., and Tybulewicz, V. L. (2010) The SYK tyrosine kinase: a crucial player in diverse biological functions. *Nat. Rev. Immunol.* **10,** 387–402 CrossRef Medline
3. Cheng, A. M., Rowley, B., Pao, W., Hayday, A., Bolen, J. B., and Pawson, T. (1995) Syk tyrosine kinase required for mouse viability and B-cell development. *Nature* **378,** 303–306 CrossRef Medline
4. Abtahian, F., Guerriero, A., Sebzda, E., Lu, M.-M., Zhou, R., Mocsai, A., Myers, E. E., Huang, B., Jackson, D. G., Ferrari, V. A., Tybulewicz, V., Lowell, C. A., Lepore, J. J., Koretzky, G. A., and Kahn, M. L. (2003) Regulation of blood and lymphatic vascular separation by signaling proteins SLP-76 and Syk. *Science* **299,** 247–251 CrossRef Medline
5. Krisenko, M. O., and Geahlen, R. L. (2015) Calling in SYK: SYK's dual role as a tumor promoter and tumor suppressor in cancer. *Biochim. Biophys. Acta* **1853,** 254–263 CrossRef
6. Streubel, B., Vinatzer, U., Willheim, M., Raderer, M., and Chott, A. (2006) Novel t(5;9)(q33;q22) fuses ITK to SYK in unspecified peripheral T-cell lymphoma. *Leukemia* **20,** 313–318 CrossRef Medline
7. Dierks, C., Adrian, F., Fisch, P., Ma, H., Maurer, H., Herchenbach, D., Forster, C. U., Sprissler, C., Liu, G., Rottmann, S., Guo, G. R., Katja, Z., Veelken, H., and Warmuth, M. (2010) The ITK-SYK fusion oncogene induces a T-cell lymphoproliferative disease in mice mimicking human disease. *Cancer Res.* **70,** 6193–6204 CrossRef Medline
8. Friedberg, J. W., Sharman, J., Sweetenham, J., Johnston, P. B., Vose, J. M., Lacasce, A., Schaefer-Cutillo, J., De Vos, S., Sinha, R., Leonard, J. P., Cripe, L. D., Gregory, S. A., Sterba, M. P., Lowe, A. M., Levy, R., and Shipp, M. A. (2010) Inhibition of Syk with fostamatinib disodium has significant clini-

cal activity in non-Hodgkin lymphoma and chronic lymphocytic leukemia. *Blood* **115,** 2578–2585 CrossRef Medline

9. Liu, D., and Mamorska-Dyga, A. (2017) Syk inhibitors in clinical development for hematological malignancies. *J. Hematol. Oncol.* **10,** 145 CrossRef Medline

10. Moroni, M., Soldatenkov, V., Zhang, L., Zhang, Y., Stoica, G., Gehan, E., Rashidi, B., Singh, B., Ozdeirli, M., and Mueller, S. C. (2004) Progressive loss of Syk and abnormal proliferation in breast cancer cells. *Cancer Res.* **64,** 7346–7354 CrossRef Medline

11. Yuan, Y., Mendez, R., Sahin, A., and Dai, J. L. (2001) Hypermethylation leads to silencing of the *SYK* gene in human breast cancer hypermethylation leads to silencing of the *SYK* gene in human breast cancer. *Cancer Res.* **61,** 5558–5561 Medline

12. Coopman, P. J. P., Do, M. T., Barth, M., Bowden, E. T., Hayes, A. J., Basyuk, E., Blancato, J. K., Vezza, P. R., McLeskey, S. W., Mangeat, P. H., and Mueller, S. C. (2000) The Syk tyrosine kinase suppresses malignant growth of human breast cancer cells. *Nature* **406,** 742–747 CrossRef Medline

13. Grädler, U., Schwarz, D., Dresing, V., Musil, D., Bomke, J., Frech, M., Greiner, H., Jäkel, S., Rysiok, T., Müller-Pompalla, D., and Wegener, A. (2013) Structural and biophysical characterization of the Syk activation switch. *J. Mol. Biol.* **425,** 309–333 CrossRef Medline

14. Tsang, E., Giannetti, A. M., Shaw, D., Dinh, M., Tse, J. K. Y., Gandhi, S., Ho, H., Wang, S., Papp, E., and Bradshaw, J. M. (2008) Molecular mechanism of the Syk activation switch. *J. Biol. Chem.* **283,** 32650–32659 CrossRef Medline

15. Bradshaw, J. M. (2010) The Src, Syk, and Tec family kinases: distinct types of molecular switches. *Cell Signal.* **22,** 1175–1184 CrossRef Medline

16. Monks, C. R. F., Freiberg, B. A., Kupfer, H., Sciaky, N., and Kupfer, A. (1998) Three-dimensional segregation of supramolecular activation clusters in T cells. *Nature* **395,** 82–86 CrossRef Medline

17. Bromley, S. K., Burack, W. R., Johnson, K. G., Somersalo, K., Sims, T. N., Sumen, C., Davis, M. M., Shaw, A. S., Allen, P. M., and Dustin, M. L. (2001) The immunological synapse. *Annu. Rev. Immunol.* **19,** 375–396 CrossRef Medline

18. Mócsai, A., Zhou, M., Meng, F., Tybulewicz, V. L., and Lowell, C. A. (2002) Syk is required for integrin signaling in neutrophils. *Immunity* **16,** 547–558 CrossRef Medline

19. Yan, S. R., Huang, M., and Berton, G. (1997) Signaling by adhesion in human neutrophils: activation of the p72^syk tyrosine kinase and formation of protein complexes containing p72^syk and Src family kinases in neutrophils spreading over fibrinogen. *J. Immunol.* **158,** 1902–1910 Medline

20. Auger, J. M., Kuijpers, M. J., Senis, Y. A., Watson, S. P., and Heemskerk, J. W. (2005) Adhesion of human and mouse platelets to collagen under shear: a unifying model. *FASEB J.* **19,** 825–827 CrossRef Medline

21. Woodside, D. G., Obergfell, A., Leng, L., Wilsbacher, J. L., Miranti, C. K., Brugge, J. S., Shattil, S. J., and Ginsberg, M. H. (2001) Activation of Syk protein tyrosine kinase through interaction with integrin β cytoplasmic domains. *Curr. Biol.* **11,** 1799–1804 CrossRef Medline

22. Woodside, D. G., Obergfell, A., Talapatra, A., Calderwood, D. A., Shattil, S. J., and Ginsberg, M. H. (2002) The N-terminal SH2 domains of Syk and ZAP-70 mediate phosphotyrosine-independent binding to integrin β cytoplasmic domains. *J. Biol. Chem.* **277,** 39401–39408 CrossRef Medline

23. Law, D. A., Nannizzi-Alaimo, L., Ministri, K., Hughes, P. E., Forsyth, J., Turner, M., Shattil, S. J., Ginsberg, M. H., Tybulewicz, V. L., and Phillips, D. R. (1999) Genetic and pharmacological analyses of Syk function in αIIbβ3 signaling in platelets. *Blood* **93,** 2645–2652 Medline

24. Hughes, C. E., Finney, B. A., Koentgen, F., Lowe, K. L., and Watson, S. P. (2015) The N-terminal SH2 domain of Syk is required for (hem) ITAM, but not integrin, signaling in mouse platelets. *Blood* **125,** 144–154 CrossRef Medline

25. Clark, E. A., Shattil, S. J., Ginsberg, M. H., Bolen, J., and Brugge, J. S. (1994) Regulation of the protein tyrosine kinase pp72^syk by platelet agonists and the integrin αIIbβ3. *J. Biol. Chem.* **269,** 28859–28864 Medline

26. Shults, M. D., Janes, K. A., Lauffenburger, D. A., and Imperiali, B. (2005) A multiplexed homogeneous fluorescence-based assay for protein kinase activity in cell lysates. *Nat. Methods* **2,** 277–283 CrossRef Medline

27. Shults, M. D., Carrico-Moniz, D., and Imperiali, B. (2006) Optimal Sox-based fluorescent chemosensor design for serine/threonine protein kinases. *Anal. Biochem.* **352,** 198–207 CrossRef Medline

28. Papp, E., Tse, J. K., Ho, H., Wang, S., Shaw, D., Lee, S., Barnett, J., Swinney, D. C., and Bradshaw, J. M. (2007) Steady state kinetics of spleen tyrosine kinase investigated by a real time fluorescence assay. *Biochemistry* **46,** 15103–15114 CrossRef Medline

29. Natsume, T., Koide, T., Yokota, S., Hirayoshi, K., and Nagata, K. (1994) Interactions between collagen-binding stress protein HSP47 and collagen: analysis of kinetic parameters by surface plasmon resonance biosensor. *J. Biol. Chem.* **269,** 31224–31228 Medline

30. Yan, B., Calderwood, D. A., Yaspan, B., and Ginsberg, M. H. (2001) Calpain cleavage promotes talin binding to the β3 integrin cytoplasmic domain. *J. Biol. Chem.* **276,** 28164–28170 CrossRef Medline

31. Schmitz, R., Baumann, G., and Gram, H. (1996) Catalytic specificity of phosphotyrosine kinases Blk, Lyn, c-Src and Syk as assessed by phage display. *J. Mol. Biol.* **260,** 664–677 CrossRef Medline

32. Fütterer, K., Wong, J., Grucza, R. A., Chan, A. C., and Waksman, G. (1998) Structural basis for Syk tyrosine kinase ubiquity in signal transduction pathways revealed by the crystal structure of its regulatory SH2 domains bound to a dually phosphorylated ITAM peptide. *J. Mol. Biol.* **281,** 523–537 CrossRef Medline

33. Ye, F., Petrich, B. G., Anekal, P., Lefort, C. T., Kasirer-Friede, A., Shattil, S. J., Ruppert, R., Moser, M., Fässler, R., and Ginsberg, M. H. (2013) The mechanism of kindlin-mediated activation of integrin αIIbβ3. *Curr. Biol.* **23,** 2288–2295 CrossRef Medline

34. Morse, E. M., Brahme, N. N., and Calderwood, D. A. (2014) Integrin cytoplasmic tail interactions. *Biochemistry* **53,** 810–820 CrossRef Medline

35. Maartens, A. P., and Brown, N. H. (2015) The many faces of cell adhesion during *Drosophila* muscle development. *Dev. Biol.* **401,** 62–74 CrossRef Medline

36. de Castro, R. O., Zhang, J., Jamur, M. C., Oliver, C., and Siraganian, R. P. (2010) Tyrosines in the carboxyl terminus regulate Syk kinase activity and function. *J. Biol. Chem.* **285,** 26674–26684 CrossRef Medline

37. Furlong, M. T., Mahrenholz, A. M., Kim, K.-H., Ashendel, C. L., Harrison, M. L., and Geahlen, R. L. (1997) Identification of the major sites of autophosphorylation of the murine protein-tyrosine kinase Syk. *Biochim. Biophys. Acta* **1355,** 177–190 CrossRef

38. Fitzgerald, D. J., Berger, P., Schaffitzel, C., Yamada, K., Richmond, T. J., and Berger, I. (2006) Protein complex expression by using multigene baculoviral vectors. *Nat. Methods* **3,** 1021–1032 CrossRef Medline

39. Gileadi, O., Burgess-Brown, N. A., Colebrook, S. M., Berridge, G., Savitsky, P., Smee, C. E., Loppnau, P., Johansson, C., Salah, E., and Pantic, N. H. (2008) High throughput production of recombinant human proteins for crystallography. *Methods Mol. Biol.* **426,** 221–246 CrossRef Medline